PAPER • OPEN ACCESS

Selection rules for breaking selection rules

New Journal of Physics
The open access journal at the forefront of physics

Deutsche Physikalische Gesellschaft DPG
IOP Institute of Physics

Published in partnership with: Deutsche Physikalische Gesellschaft and the Institute of Physics

OPEN ACCESS

RECEIVED
8 June 2021

REVISED
11 September 2021

ACCEPTED FOR PUBLICATION
17 September 2021

PUBLISHED
1 November 2021

PAPER

Selection rules for breaking selection rules

Matan Even Tzur[1,*], Ofer Neufeld[1,2], Avner Fleischer[3] and Oren Cohen[1]

[1] Solid State Institute and Physics Department, Technion—Israel Institute of Technology, 3200003, Haifa, Israel
[2] Theory Department, Max Planck Institute for the Structure and Dynamics of Matter, Hamburg 22761, Germany
[3] Raymond and Beverly Sackler Faculty of Exact Science, School of Chemistry and Center for Light Matter Interaction, Tel Aviv University, 6997801, Tel Aviv, Israel
[*] Author to whom any correspondence should be addressed.

E-mail: Matanev@campus.technion.ac.il

Keywords: selection rules, high harmonic generation, Floquet group theory, dynamical symmetry, symmetry breaking, Floquet perturbation theory

Supplementary material for this article is available online

Abstract

Floquet systems often exhibit dynamical symmetries (DS) that govern the time-dependent dynamics and result in selection rules. When a DS is broken, selection rule deviations are expected. Typically, information about the symmetry-breaking perturbation/phase and the time-dependent dynamics can be extracted from these deviations, hence they are regarded as a background free gauge of symmetry breaking. However, to date, DS breaking & selection rule deviations are not described by a general approach, thus there is no universal insight about the interplay between selection rule deviations, the symmetry breaking perturbation, and the broken DS. Here we consider DS breaking in Floquet systems from a general standpoint, formulating a general theory that analytically connects the symmetry-broken and fully symmetric systems. Using an external laser (of arbitrary frequency and polarization), as a model DS breaking perturbation, we discover that the broken symmetry systematically imposes selection rules on the symmetry-broken system, which physically manifest as scaling laws of selection rule deviations. We term these rules 'selection rules for breaking selection rules'—a new concept in physics. We numerically validate the analytical theory in the context of high harmonic generation. Our discovery is a general feature of nonlinear wave-mixing phenomena, and we expect it to apply to any Floquet system (classical & quantum) and to any DS breaking mechanism (either by intrinsic or extrinsic elements of the system).

1. Introduction

Floquet systems, i.e. systems described by a time-periodic Hamiltonian, are widespread in nonlinear optics and many other fields of physics [1–8]. When they exhibit spatio-temporal symmetries (denoted dynamical symmetries, DS), selection rules are obtained [9–12]. For instance, in high harmonic generation (HHG), DS are known to dictate selection rules resulting in forbidden harmonics and polarization restrictions [9, 10, 12], e.g. a counter-rotating ω–2ω bi-circular field interacting with an isotropic medium results in forbidden optical emission of $3n$ harmonics (where n is an integer number) of the fundamental driver [13–15]. However, if the system's symmetry is slightly broken by some perturbation, previously forbidden dynamics (e.g. optical emissions of certain frequencies) become slightly allowed. But how much is 'slightly'? How do selection rule deviations (and other observables) scale with the strength of the perturbation as the system transitions from being symmetric to asymmetric? Furthermore, to what extent is the broken-symmetry relevant in the symmetry-broken system? And how is the interplay between the broken symmetry and the symmetry-breaking perturbation related to selection rule deviations? The significance of a general answer to these questions, namely, a general quantitative formalism that systematically describes DS breaking, is fundamental, as DS breaking is a reoccurring theme in nonlinear spectroscopy. For example,

symmetry broken HHG serves as a key phenomenon in ultrafast symmetry breaking spectroscopy of molecular symmetry [16], orientation [17, 18], chirality [19], electric currents [20], imaging of microscopic electric field distributions [21], and detection of topological phase transitions [22]. Typically, such experiments start with the system possessing a DS, forcing the HHG spectrum to adhere to symmetry-induced selection rules. When the DS is broken, the HHG spectrum displays selection rule deviations and the sought upon measurement (the degree of symmetry breaking) is inferred from these deviations via an analytical mapping. For example, even harmonics are forbidden when an ensemble of randomly-aligned molecules is driven by a linearly-polarized driver [9]. When the molecules are impulsively oriented by a pump laser pulse, the DS is broken and even harmonics are generated. The ensemble's degree of orientation can be extracted from the intensities of even harmonics [18]. Selection-rule deviations are especially appealing for spectroscopy because they are a background-free gauge of symmetry breaking, enabling high precision measurement of complex dynamics with *fs* temporal resolution and a relatively simple experimental technique. Still, despite their great utility and fundamental importance, the interplay between selection rule deviations and DS-breaking was not investigated from a general perspective, and was only considered in several ad-hoc situations [16–24]. Thus, it remains unknown if any general insight about this interplay can be obtained, and if so, what it is.

Motivated to bridge this gap, we present a general analysis of DS-breaking and selection-rule-deviations in Floquet systems & nonlinear optics. Notably, we present a new concept: selection rules for breaking selection rules—these are rules that describe the allowed and forbidden behavior of selection rule deviations. Using a laser of arbitrary polarization and frequency as a model symmetry breaking perturbation, we perform a general analytical analysis of the interplay between selection rule deviations, the broken symmetry, and the perturbation itself. Our analysis utilizes Floquet perturbation theory (FPT [25]) to expand the spectral components of an expectation value of interest to a polynomial in the perturbation strength, without assuming anything about the unperturbed system, except for its initial DS. Remarkably, we find that the DS of the unperturbed system (the broken symmetry) imposes selection rules on the coefficients of the polynomial, which dictate the characteristic behavior of the system as it transitions from fully symmetric to symmetry-broken. That is, we discover that the broken symmetry imposes selection rules on the symmetry-broken system. We term the new concept of selection rules imposed by broken symmetries 'selection rules for breaking selection rules', and formally derive and tabulate them for all DSs in $(2+1)$D Floquet systems. As an example, we apply our approach to nonlinear optics, focusing on HHG driven by a laser with polarization components that break the symmetry. We present numerical examples that show that our analytical approach correctly predicts the scaling of the HHG emission with the amplitude and polarization of a symmetry-breaking perturbation, and that different DSs break differently by an identical perturbation. We stress that selection rules for breaking selection rules is a general new concept that should exist in any non-linear wave-mixing phenomenon, be it matter waves, acoustic waves, etc. Furthermore, the explicit rules we have derived for a symmetry breaking laser, are also useful for the analysis of DS breaking by other symmetry breaking perturbations, because often, time periodic perturbations can be reformulated as effective gauge fields [26, 27].

This paper is organized as follows: first, we show how selection rules for breaking selection rules emerge upon breaking the symmetry with an external perturbation, and tabulate the rules imposed by a perturbative monochromatic laser field. Then, we present numerical explorations of the HHG emission scaling in the presence perturbations and show that the results match very well to the analytical predictions of our theory. Finally, we summarize our results and discuss potential implications.

2. Selection rules for breaking selection rules

We begin by considering how DS breaking by a perturbing laser modifies the expectation values of a general Floquet system at hand. We focus on the dipole moment expectation value since it naturally relates to the optical emission of the system and subsequently to the analysis of HHG in the next section. The results for other expectation values/perturbations may be obtained by analogous derivations.

Consider a $(2+1)$D Floquet system, with the time-periodic Hamiltonian $\hat{H}_0(t) = \hat{H}_0(t+T)$ whose fundamental frequency is $\omega = 2\pi/T$. In the following, we calculate the perturbative corrections to the $n\omega$ frequency components of the dipole moment expectation value, induced by a perturbation of frequency $s\omega$ (both n and s are integers). The Floquet Hamiltonian is defined by $\hat{\mathcal{H}}_f = \hat{H}_0 - i\partial_t$. It is eigenfunctions $|\phi_{\alpha(0)}(t)\rangle$and eigenvalues $\varepsilon_{\alpha(0)}$ are the Floquet states, and quasi energies, respectively (the subscript (0) indicates a non-perturbed quantity, and α indicates the Floquet state index). When $\hat{H}_0(t)$ exhibits some DS, the optical emission of any single state $|\phi_{\alpha(0)}(t)\rangle$ is subject to corresponding polarization restrictions and harmonic generation selection rules. When $\hat{H}_0(t)$ is perturbed by a symmetry breaking perturbation $\lambda\hat{W}(t) = \lambda\hat{W}(t+T)$, the state $|\phi_{\alpha(0)}(t)\rangle$ is modified to $|\phi_\alpha(\lambda, t)\rangle$. Note that the perturbed system is under

the effect of two driving fields—a symmetry preserving pump field (or a different periodic excitation) and a symmetry breaking perturbing field. The expectation values from the modified state $|\phi_\alpha(\lambda,t)\rangle$ exhibits selection rule deviations. For example, if $\hat{H}_0(t)$ is perturbed by an electric field of amplitude λ, polarization $\mathbf{p}$ and frequency $s\omega$, where $\omega = 2\pi/T$ and s may be any integer (extensions to any rational number $s = r/q$ are discussed in the SI (https://stacks.iop.org/NJP/23/103039/mmedia, section 4), then within the electric dipole approximation, the modified Hamiltonian is $\hat{H} = \hat{H}_0 + \lambda\hat{W}(t)$ where:

$$\lambda\hat{W}(t) = \lambda\Re\left\{\mathbf{p}\cdot\hat{\boldsymbol{\mu}}e^{is\omega t}\right\}, \tag{1}$$

and where $\hat{\boldsymbol{\mu}}$ is the electric dipole moment operator such that:

$$\mathbf{p}\cdot\hat{\boldsymbol{\mu}} = p_x x + p_y y, \tag{2}$$

where x, y are Cartesian spatial coordinates. The $n\omega$ (where n is an integer) frequency component of the dipole moment expectation value $\hat{\boldsymbol{\mu}}(\lambda)$ is given by

$$\widetilde{\boldsymbol{E}}(\lambda,n\omega) = \int_0^T \frac{\mathrm{d}t}{T}\langle\phi_\alpha(\lambda,t)|\,\hat{\boldsymbol{\mu}}e^{in\omega t}\,|\phi_\alpha(\lambda,t)\rangle. \tag{3}$$

Using FPT, we expand $|\phi_\alpha(\lambda,t)\rangle$ to 1st order in λ, and subsequently $\widetilde{\boldsymbol{E}}(\lambda,n\omega)$ to a quadratic polynomial in λ

$$\widetilde{\boldsymbol{E}}(\lambda,n\omega) = \widetilde{\boldsymbol{E}}_0(n\omega) + \lambda\widetilde{\boldsymbol{E}}_1(n\omega) + \lambda^2\widetilde{\boldsymbol{E}}_2(n\omega). \tag{4}$$

The term $\widetilde{\boldsymbol{E}}_0(n\omega)$ complies with any selection rules imposed by the DSs of the unperturbed system, which are derived in [12]. The new contributions $\widetilde{\boldsymbol{E}}_1(n\omega), \widetilde{\boldsymbol{E}}_2(n\omega)$ are a result of the perturbation, inducing selection rule deviations that scale linearly and quadratically with the perturbation strength, respectively. The explicit forms of $\widetilde{\boldsymbol{E}}_0(n\omega), \widetilde{\boldsymbol{E}}_1(n\omega)$ and $\widetilde{\boldsymbol{E}}_2(n\omega)$ (defined in equations (3) and (4)) are given by (see SI, section 1 for full derivation):

$$\widetilde{\boldsymbol{E}}_0(n\omega) = \mathbf{F}_n^{\alpha\alpha} \tag{5}$$

$$\widetilde{\boldsymbol{E}}_1(n\omega) = \sum_{\substack{(\beta,m)\neq(\alpha,0)\\ g=\pm1}} \frac{\left(\mathbf{p}_g\cdot\mathbf{F}^{\beta\alpha}_{\mathrm{gs}-m}\right)\mathbf{F}^{\alpha\beta}_{n+m} + \left(\mathbf{p}_g\cdot\mathbf{F}^{\alpha\beta}_{m-\mathrm{gs}}\right)\mathbf{F}^{\beta\alpha}_{n-m}}{\varepsilon_{\alpha(0)} - \varepsilon_{\beta(0)} - m\omega} \tag{6}$$

and

$$\widetilde{\boldsymbol{E}}_2(n\omega) = \frac{1}{4}\sum_{\substack{(\beta,m)\neq(\alpha,0)\\ (\kappa,l)\neq(\alpha,0)\\ g_1,g_2=\pm1}} \frac{\left(\mathbf{p}_{g_1}\cdot\mathbf{F}^{\alpha\kappa}_{l-g_1 s}\right)\left(\mathbf{p}_{g_2}\cdot\mathbf{F}^{\beta\alpha}_{g_2 s-m}\right)\mathbf{F}^{\kappa\beta}_{n+m-l}}{\left(\varepsilon_{\alpha(0)} - \varepsilon_{\kappa(0)} - l\omega\right)\left(\varepsilon_{\alpha(0)} - \varepsilon_{\beta(0)} - m\omega\right)} \tag{7}$$

Here, $s\omega$ is the frequency of the perturbation (equation (1)), α and β are Floquet state indices, the quasi-energies $\varepsilon_{\alpha(0)}$ are defined by $\hat{\mathcal{H}}_f|\phi_{\alpha(0)}\rangle = \varepsilon_{\alpha(0)}|\phi_{\alpha(0)}\rangle$, $\mathbf{p}_g \equiv \Re\{\mathbf{p}\} + ig\Im\{\mathbf{p}\}$ and $\mathbf{F}_n^{\beta\alpha}$ is the $n\omega$ frequency component of the time-dependent matrix element $\langle\phi_{\beta(0)}|\hat{\boldsymbol{\mu}}|\phi_{\alpha(0)}\rangle$:

$$\langle\phi_{\beta(0)}\,|\hat{\boldsymbol{\mu}}|\,\phi_{\alpha(0)}\rangle = \sum_n \mathbf{F}_n^{\beta\alpha}e^{i\omega nt} \tag{8}$$

Equations (5)–(8) provide a quantitative analytical description for the scaling of the selection rule deviations (and the spectrum in general) up to the wavefunction normalization, and the additional higher order contributions, which may be introduced by the 2nd order correction to the wavefunction. We shall now examine how the broken symmetry imposes different selection rules on $\widetilde{\boldsymbol{E}}_0(n\omega), \widetilde{\boldsymbol{E}}_1(n\omega)$ and $\widetilde{\boldsymbol{E}}_2(n\omega)$. $\widetilde{\boldsymbol{E}}_0(n\omega) = \mathbf{F}_n^{\alpha\alpha}$ exhibits selection rules because it is calculated directly from an eigenstate of the symmetric system [12]. Similarly, the matrix elements $\mathbf{F}_n^{\beta\alpha}$ also exhibit (other) selection rules because they are calculated directly from symmetric Floquet states. As the elements $\mathbf{F}_n^{\beta\alpha}$ are the building blocks of $\widetilde{\boldsymbol{E}}_1(n\omega), \widetilde{\boldsymbol{E}}_2(n\omega)$, they also exhibit selection rules—selection rules for breaking selection rules. For example, we derive here these selection rules for a time reversal ($\hat{T}$) symmetric system, perturbed by a linearly polarized laser, i.e. $\mathbf{p}\in\mathbb{R}^2$ is real. Since the unperturbed system is $\hat{T}$ symmetric, the unperturbed Floquet states are eigenfunctions of $\hat{T}$ whose eigenvalues are either $+1$ or -1. By operating with $\hat{T}$ on equation (8) we find that $\pm\mathbf{F}_n^{\beta\alpha} = \mathbf{F}_n^{\beta\alpha}$, where a plus (minus) sign is used when $|\phi_{\alpha(0)}\rangle$ and $|\phi_{\beta(0)}\rangle$ have the same (different) $\hat{T}$ eigenvalue. Therefore, if the α and β Floquet states have the same (different) eigenvalue, $\mathbf{F}_n^{\beta\alpha}$ is real (imaginary). Thus, all the contributions to equation (6) are real, i.e. $\widetilde{\boldsymbol{E}}_1(n\omega)$ is real. In other words,

Table 1. Selection rules for breaking selection rules by a linearly polarized monochromatic laser. The broken symmetry imposes universal selection rules on $\widetilde{\boldsymbol{E}}_{0,1,2}(n\omega)$, which also depend on the polarization ($\boldsymbol{p}$) and frequency ($s\omega$) of the perturbation. The selection rules for $\widetilde{\boldsymbol{E}}_0(n\omega)$ were tabulated in [12] and the selection rules for $\widetilde{\boldsymbol{E}}_{1,2}$ are derived in the SI, section 2.

Dynamical symmetry	Selection rules & selection rules for breaking selection rules		
	Time-reversal symmetries		
$\hat{T}$	$\widetilde{\boldsymbol{E}}_0(n\omega)\in \mathrm{R}^2$	$\widetilde{\boldsymbol{E}}_1(n\omega)\in \mathrm{R}^2$	$\widetilde{\boldsymbol{E}}_2(n\omega)\in \mathrm{R}^2$
$\hat{Q}$	$\widetilde{\boldsymbol{E}}_0(n\omega)\in i\mathrm{R}^2$	$\widetilde{\boldsymbol{E}}_1(n\omega)\in \mathrm{R}^2$	$\widetilde{\boldsymbol{E}}_2(n\omega)\in i\mathrm{R}^2$
$\hat{G}$	$\widetilde{\boldsymbol{E}}_0(n\omega)\in i^{n+1}\mathrm{R}^2$	$\widetilde{\boldsymbol{E}}_1(n\omega)\in i^{n+s}\mathrm{R}^2$	$\widetilde{\boldsymbol{E}}_2(n\omega)\in i^{n+1}\mathrm{R}^2$
	Dynamical reflection symmetries		
$\hat{D}_y$	$\widetilde{E}_{0x}, i\widetilde{E}_{0y}\in i\mathrm{R}$	$\widetilde{E}_{1x}(n\omega), i\widetilde{E}_{1y}(n\omega)\in p_x\mathrm{R}+ip_y\mathrm{R}$	$\widetilde{E}_{2x}(n\omega), i\widetilde{E}_{2y}(n\omega)\in ip_x^2\mathrm{R}+ip_y^2\mathrm{R}+p_xp_y\mathrm{R}$
$\hat{H}_y$	$\widetilde{E}_{0x}(n\omega), i\widetilde{E}_{0y}(n\omega)\in i^{n+1}\mathrm{R}$	$\widetilde{E}_{1x}(n\omega), i\widetilde{E}_{1y}(n\omega)\in i^{n+s}p_x\mathrm{R}+i^{n+s+1}p_y\mathrm{R}$	$\widetilde{E}_{2x}(n\omega), i\widetilde{E}_{2y}(n\omega)\in i^{n+1}p_x^2\mathrm{R}+i^{n+1}p_y^2\mathrm{R}+i^np_xp_y\mathrm{R}$
$\hat{Z}_y$	$\widetilde{\boldsymbol{E}}_0(n\omega)\in \begin{pmatrix}0&1\\1&0\end{pmatrix}^n\begin{pmatrix}1&0\\0&0\end{pmatrix}\mathrm{C}^2$	$\widetilde{\boldsymbol{E}}_1(n\omega)\in \begin{pmatrix}0&1\\1&0\end{pmatrix}^{n+s}\begin{pmatrix}p_x&0\\0&p_y\end{pmatrix}\mathrm{C}^2$	$\widetilde{\boldsymbol{E}}_2(n\omega)\in \begin{pmatrix}0&1\\1&0\end{pmatrix}^n\begin{pmatrix}p_xp_y&0\\0&p_x^2+\alpha p_y^2\end{pmatrix}\mathrm{C}^2;\alpha\in\mathrm{C}$
	Rotational & elliptical dynamical symmetries		
$\hat{C}_{N,M}$	$\widetilde{\boldsymbol{E}}_0(n\omega)\neq 0$ for	$\widetilde{\boldsymbol{E}}_1(n\omega)\neq 0$ for	$\widetilde{\boldsymbol{E}}_2(n\omega)\neq 0$ for
$\hat{e}_{N,M}$	$n=Nm\pm M$	$n=Nm\pm(1\pm1)M\pm s$	$n=Nm\pm(2\pm1)M\pm(1\pm1)s$

$\widetilde{\boldsymbol{E}}_1(n\omega)$ is linearly polarized and in phase with the perturbation. Similarly, $\widetilde{\boldsymbol{E}}_2(n\omega)$ is real since each contribution to the summation (equation (7)) is comprised of a multiplication of either three real entities, or two imaginary entities and one real entity. Overall, for $\hat{T}$ symmetry we conclude that both $\widetilde{\boldsymbol{E}}_1(n\omega)$ and $\widetilde{\boldsymbol{E}}_2(n\omega)$ are real, hence they are linearly polarized and in phase with the perturbation (yet not necessarily polarized along the same axis). We emphasize this important result—corrections to the light emission/observable that arise from the time-dependent perturbation to the initial system have a restricted form that arises from the symmetry of the unperturbed system and the properties of the perturbation. These are selection rules to the breaking of the initial selection rule of the unperturbed system, which are in close analogy with the selection rules of the symmetric system.

The derivations for all other DSs are based on similar arguments (presented in the SI, section 2) and their results are summarized in table 1. The different DS operations are explicitly defined in the SI and in [12]. These selection rules form a general platform for symmetry breaking spectroscopy in Floquet systems. Table 1 accounts for linearly polarized perturbations, but the same approach could be utilized to account for any other polarization (for example, see another explicit table for circularly polarized perturbing fields in the SI, section 3). At this point, it is worth mentioning again that we utilized here non-degenerate perturbation theory and that these selection rules only describe the scaling of the emission of each separate Floquet state. When the system is initially in a superposition of several Floquet states, the emission may scale differently because the interference between the states introduces additional terms in equation (4). However, these terms can also be accounted for with the same approach. In fact, one may utilize this property to probe interferences between Floquet states. We also note that the selection rules for symmetries that involve the time-reversal operation were derived under the assumption that the quasi-energy spectrum is real valued. Finally, we note that by expanding the Floquet state to 1st order in λ, the presented treatment does not immediately account the quadratic contribution originating from the 2nd order Floquet state correction. However, we have verified that this contribution exhibits the same selection rules for breaking selection rules hence the approach is consistent in describing the scaling of a physical signal.

Before moving on to discuss explicit examples, it is instructive to discuss the physical meaning and structure of the results in table 1. Since the perturbation polarization vector was real in the derivation of table 1, real quantities are in equal or opposite phase with respect to the perturbation, and imaginary quantities have $\pm\pi/2$ phase shifts relative to the perturbation. A complex quantity has an unrestricted phase. The x and y polarization components of $\widetilde{\boldsymbol{E}}_i$ ($i=0,1,2$) are denoted by $\widetilde{E}_{ix}$ and $\widetilde{E}_{iy}$ respectively. If both of these components are in phase, the contribution $\widetilde{\boldsymbol{E}}_i$ is linearly polarized. For example, for $\hat{Q}$ DS, $\widetilde{\boldsymbol{E}}_1(n\omega)\in \mathrm{R}^2$ is linearly polarized and in equal/opposite phase with the perturbation, whereas $\widetilde{\mathbf{E}}_{0,2}(n\omega)\in i\mathrm{R}^2$ are linearly polarized and have a $\pm\pi/2$ phase shifts relative to the perturbation. It is important to emphasize that $\widetilde{\mathbf{E}}_0$ and $\widetilde{\mathbf{E}}_{0,2}$, are not necessarily linearly polarized along the same axis. Rules that depend on p_x and p_y restrict the scaling of a particular expectation value with these quantities, and the phase of each component in the scaling. For example, for $\hat{D}_y$ DS, we obtained that $\widetilde{E}_{1x}(n\omega)\in p_x\mathrm{R}+ip_y\mathrm{R}$, which means that for the x-polarization component of harmonic n, there are two linearly scaling components—one that depends linearly on p_x and is in equal/opposite phase with the perturbation, and one that depends linearly on p_y, and has a phase of $\pm\pi/2$ relative to the perturbation. Similarly, we found that the $\hat{y}$ polarized linearly scaling component of harmonic n follows $i\widetilde{E}_{1y}(n\omega)\in p_x\mathrm{R}+ip_y\mathrm{R}$, hence it is a

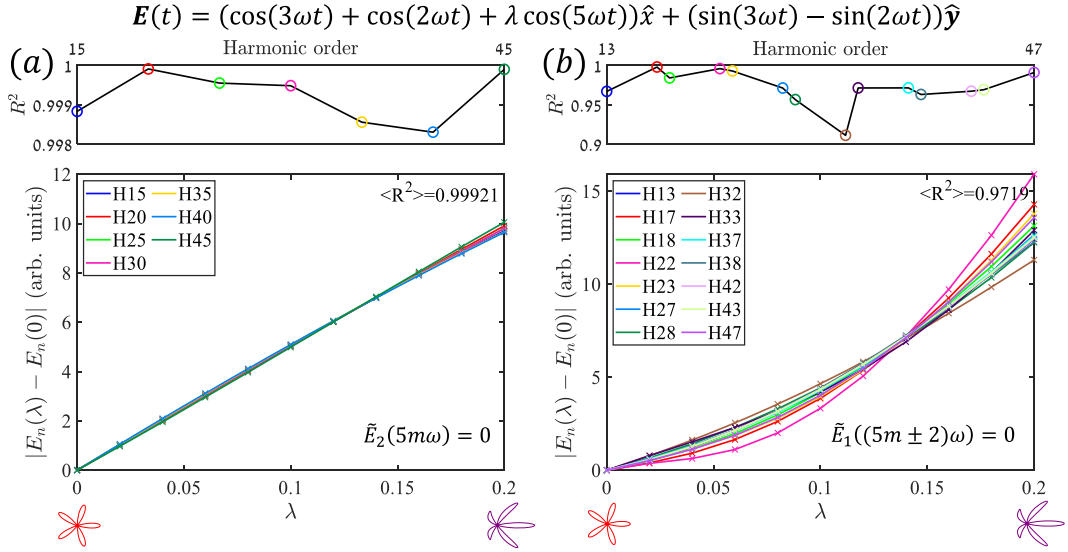

Figure 1. Numerical demonstration of selection rules for breaking $\hat{C}_{5,3}$ selection rules in HHG by an $\hat{X}$-polarized perturbative electric field of amplitude λ. For $\lambda = 0$, the Lissajous curve of the driving field is given in red. Due to the $\hat{C}_{5,3}$ DS, $5m$ harmonics are forbidden and $5m \pm 3$ are circularly polarized. For $\lambda > 0$ (purple Lissajous curve) an $\hat{X}$ polarized laser breaks the DS and induces (a) linear scaling of $5m$ harmonics (b) quadratic scaling of $5m \pm 2$ harmonics. The scaling of the harmonic amplitudes with perturbation strengths are presented in color, and the individual R^2 values are marked with the corresponding color above each subfigure. Each harmonic amplitude is multiplied by a factor such that all the harmonics fit to the graph.

sum of an equal/opposite phase component that scales linearly with p_x, and a component that scales linearly with p_y with a phase $\pm\pi/2$ relative to the perturbation. In matrix-form rules, $\widetilde{\boldsymbol{E}}_{\boldsymbol{i}} = \left(\widetilde{E}_{ix}, \widetilde{E}_{iy}\right)^{\mathrm{T}}$ where T is the transpose operation. For example, for $\hat{Z}_y$ symmetry, $\widetilde{E}_{1x}(n\omega)$ scales linearly with p_x if $n + s$ is even, or linearly with p_y if $n + s$ is odd. For $\widetilde{E}_{1y}(n\omega)$, the conditions are reversed. Both $\widetilde{E}_{1x}(n\omega)$ and $\widetilde{E}_{1y}(n\omega)$ have unrestricted phases as denoted by the multiplication C^2. Finally, the laws for rotational and elliptical DSs forbid each of the components $\widetilde{\boldsymbol{E}}_{0,1,2}(n\omega)$ to be nonzero unless n is in a specific subset of the integers. An explicit example of this selection rule for $\hat{C}_{5,3}$ symmetry follows in the next section.

3. High-harmonic-generation

Next, we explore the applicability of our approach to HHG symmetry breaking spectroscopy [16, 17, 19–22]. Within this technique, an intense laser pulse is focused into a gas, liquid, or solid target, resulting in the generation of high harmonics of the driver laser field [28]. If the driving laser is switched on slowly enough (which is most often the case in HHG experiments), the state of the system adiabatically evolves from the ground state to a single resonant (non-Hermitian) Floquet state [29]. Hence, the response of the HHG spectrum to a perturbative symmetry breaking electric field (equation (1)) is given by equation (4) and table 1.

As a first example, we consider the HHG spectra emitted from a Ne atom in an unperturbed symmetric potential well, $V_{\mathrm{Ne}}(\vec{r})$ (see methods for the explicit expression), irradiated by a counter rotating bi-circular 2ω–3ω field where ω corresponds to a wavelength of 800 nm. The Lissajous curve of this unperturbed field is given figure 1 (red, below $\lambda = 0$). The Floquet Hamiltonian describing this process exhibits a 5th order rotational DS, denoted $\hat{C}_{5,3} = \hat{\tau}_5 \cdot \hat{R}_{5,3}$, where $\hat{\tau}_5$ is $T/5$ time translation, and $\hat{R}_{5,3}$ is spatial rotation by $3 \times 2\pi/5$ (see SI, section 2, for a more detailed description of the different symmetry operations used). Thus, only $(5m \pm 3)\,\omega$ harmonic photons are emitted [12]. When we perturb the Hamiltonian with a weak linearly polarized field of amplitude λ, frequency 5ω that is linearly polarized along the x-axis ($p_x = 1, p_y = 0, s = 5$) the DS is broken, and all harmonic orders are allowed. Figure 1 shows the explicit expression for the perturbed field as a function of λ, and its Lissajous curve for $\lambda = 0$ (red) and $\lambda = 0.2$ (purple). Using table 1, we find that $\widetilde{\boldsymbol{E}}_1((5m \pm 2)\,\omega) = \widetilde{\boldsymbol{E}}_2(5m\omega) = 0$, where m is an integer. Hence, $5m$ harmonics are predicted to scale linearly with λ and $5m \pm 2$ harmonics are predicted scale quadratically (for integer m).

Figure 1 presents the scaling of the deviations for peak harmonic amplitudes of harmonics 13–47 vs λ, calculated by directly solving the time-dependent Schrödinger equation (TDSE) for this model atom (for numerical details see methods). Lower and higher order harmonics were excluded due to a low signal to

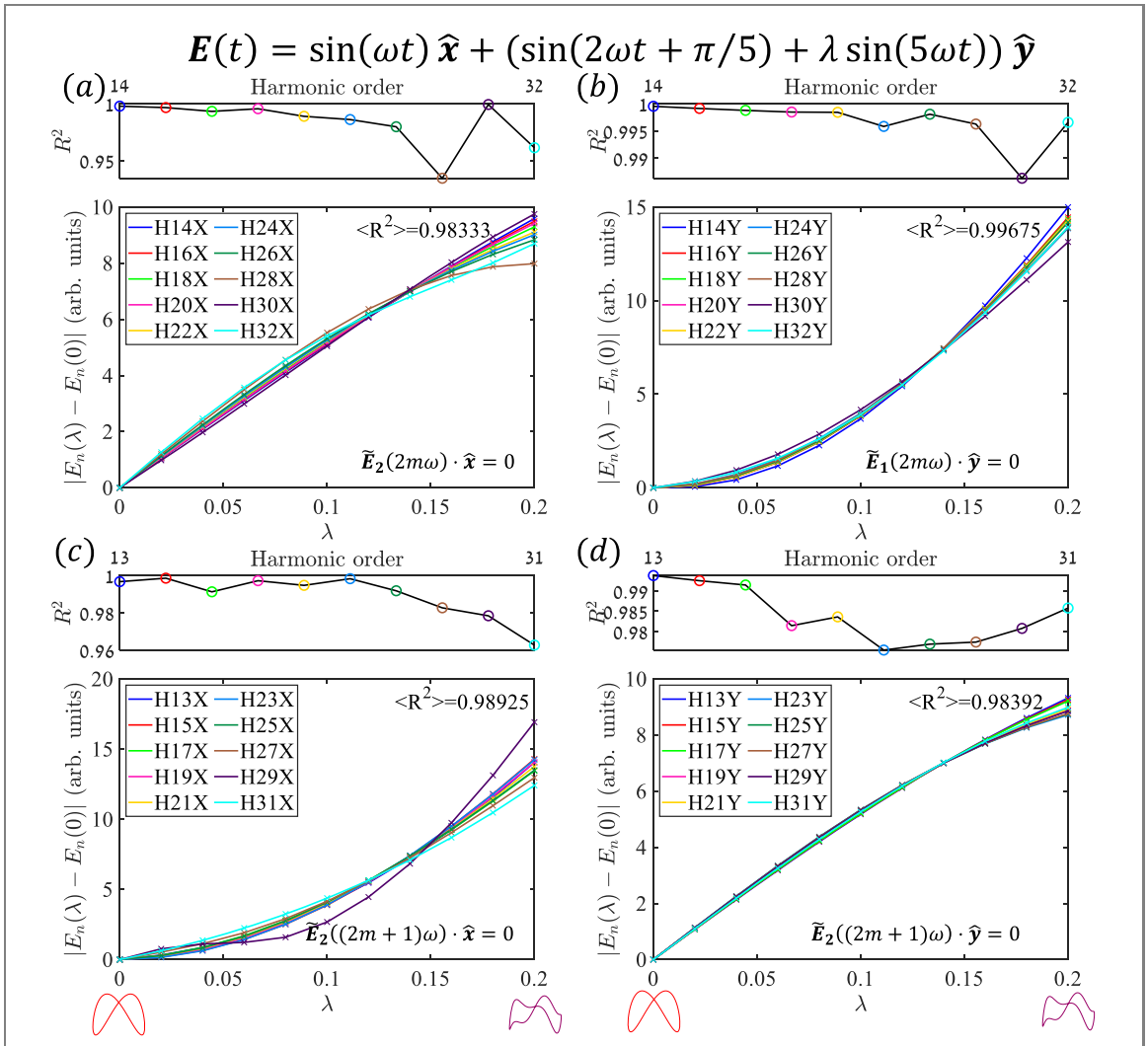

Figure 2. Numerical demonstration of selection rules for breaking $\hat{Z}_Y = \hat{\tau}_2 \cdot \hat{\sigma}_Y$ selection rules in HHG by a $\hat{Y}$-polarized perturbative electric field of amplitude λ. For $\lambda = 0$ the Lissajous curve of the driving field is given in red, and due to the $\hat{Z}_Y$ DS, $\hat{X}$ polarized $2m$ harmonics and $\hat{Y}$ polarized $2m+1$ harmonic are forbidden. For $\lambda > 0$ (purple Lissajous curve), a $\hat{Y}$ polarized electric field breaks the DS and induces (a) and (d) linear scaling of $\hat{X}(\hat{Y})$ polarized even (odd) harmonics (b) and (c) quadratic scaling of $\hat{Y}(\hat{X})$ polarized even (odd) harmonics.

noise ratio, causing their scaling to be strongly affected by the nonlinear scaling of the background radiation, which is not accounted for in Floquet theory. The signal to noise ratio of the presented (plateau) harmonics is relatively constant, but oscillations of this value do occur due to interferences of short and long electronic trajectories. The oscillations of the signal to noise ratio with harmonic order change the relative contribution of the background radiation to the scaling of the harmonics. For harmonics with a particularly low signal to noise ratio, such as harmonic 32 in figure 1(b), the analytically predicted scaling is altered by the scaling of the background, so that the value of R^2 is diminished to 0.9. However, this effect is relatively weak and the analytical predictions are numerically observed with an average $R^2 > 0.97$ for both cases.

As a second example, we consider an $\omega - 2\omega$ cross-linear driving field, which exhibits a reflection DS denoted $\hat{Z}_y = \hat{\tau}_2 \cdot \hat{\sigma}_y$, where $\hat{\sigma}_y$ is reflection relative to $\hat{\boldsymbol{y}}$ [12, 30]. The explicit expression and Lissajous curve for the driving field are given in figure 2. For $\lambda = 0$, only $\hat{x}$-polarized ($\hat{y}$-polarized) $2m \pm 1$ ($2m$) harmonics are allowed due to the $\hat{Z}_y$ DS (for integer m) [12]. When we perturb the Hamiltonian with a weak field of frequency 5ω, linearly polarized along $\hat{y}$ ($p_x = 0, p_y = 1, s = 5$) $\hat{Z}_y$ DS is broken, and all harmonic polarizations are allowed. From table 1 we find that $\widetilde{E}_{2x}(2m\omega)$, $\widetilde{E}_{1y}(2m\omega)$, $\widetilde{E}_{2y}((2m \pm 1)\omega)$, $\widetilde{E}_{1x}((2m \pm 1)\omega)$ are all equal to zero ($\widetilde{E}_{ix}, \widetilde{E}_{iy}$ are the x and y components of $\widetilde{\boldsymbol{E}}_{\mathbf{i}}$). Therefore, $2m$ harmonics are predicted to scale linearly (quadratically) with λ if polarized along $\hat{x}$ ($\hat{y}$), and $2m \pm 1$ harmonics are predicted to scale linearly (quadratically) with λ if polarized along $\hat{y}$ ($\hat{x}$) (for integer m). Figure 2 presents the amplitudes of the $\hat{x}$ and $\hat{y}$ polarization components of harmonics 13–32 vs λ (other harmonics were excluded as above). Again, the analytical predictions derived by FPT are numerically observed, with an average $R^2 > 0.95$ for all cases. Notably, the same results are obtained also when a finite

bandwidth around each harmonic is considered (see SI, section 4), i.e. this is a robust result. We note that this analysis describes a physical situation that is often encountered in HHG experiments—imperfect polarization in the driving laser field, where deviations from the desired polarization can be modeled as small perturbations. Our analysis can therefore be directly utilized to comprehensively explore symmetry breaking in standard HHG setups (e.g. as described in [31]). That is, it can be used to determine the source of symmetry breaking—imperfections in experimental conditions, or other, by measuring the scaling of the signal with a particular degree of freedom.

4. Discussion

To summarize, we have formulated a general theoretical framework that describes DS breaking in Floquet systems. Within this framework, we analyzed the scaling of the system's expectation values with a symmetry breaking perturbation and discovered that the broken symmetry systematically imposes selection rules on the symmetry broken system. These selection rules dictate the allowed/forbidden components in the scaling of the emission, as well as phase relations between different components. We termed the derived rules 'selection rules for breaking selection rules' and tabulated them according to the symmetry that imposes them. We observed numerically the validity of the derived scaling laws by examining HHG symmetry-breaking spectroscopy with different types of perturbations. Thus, the analytical theory's predictions are robust, and provide a universal framework for analyzing various, up to now disconnected, symmetry breaking mechanisms.

The discovered universal rules provide a theoretical foundation for existing HHG symmetry breaking schemes that should be useful in developing new ultrafast spectroscopic tools. It allows one to quickly characterize the response of any general system to a degree of freedom by performing a small number of calibration measurements. For instance, we have already showed here that the theory is useful for analyzing symmetry-breaking due to imperfect polarization components in the driving laser, but it can similarly (and easily) be applied to other types of symmetry breaking due to intrinsic properties of the medium (e.g. spin-orbit coupling [32]), or properties of the light-matter dressed system. In particular, by reformulating material excitations as effective gauge potentials, we expect that our approach can be extended to describe phonon-induced phase transitions [27, 33] and DS breaking in the presence of two-dimensional magnons [34]. Thus, we believe that this work will also have implications in various fields of physics beyond nonlinear optics and HHG, as well as motivate more investigations on selection rules for breaking selection rules in other systems.

5. Methods

The HHG spectra for the different cases analyzed in the paper were obtained by numerically solving the time dependent Schrodinger equation (TDSE) for an atom irradiated by a laser field, in the length gauge. The TDSE was solved on a two dimensional Cartesian grid. The TDSE, given in atomic units within the dipole approximation is:

$$\mathrm{i}\frac{\partial}{\partial t}\psi\left(t,x,y\right)=\left[-\frac{1}{2}\nabla^{2}+V\left(r\right)+V_{ab}\left(r\right)+\vec{r}\cdot\vec{E}\left(r,t\right)\right]\left|\psi\left(t,x,y\right)\right\rangle, \tag{9}$$

where $\vec{E}\left(r,t\right)$ is the laser electric field, and $V\left(r\right)$ is the atomic potential, modeled as a softened coulomb potential:

$$V\left(r\right)=-\frac{1}{\sqrt{r^{2}+a}}. \tag{10}$$

The parameter a is set to $a=0.1195$ a.u., to match the ionization potential of Ne, that is $I_{\mathrm{p}}=0.7924$ hartree [35]. $V_{ab}\left(r\right)$ is a complex absorbing potential, that was included in the equation to avoid nonphysical reflections of the wavefunction from the grid boundaries:

$$V_{ab}\left(r\right)=\begin{cases}-i5\times10^{-4}(r-r_{0})^{3}, & r\geqslant r0\\ 0, & \text{otherwise}\end{cases} \tag{11}$$

where $r_0=36$ bohr for 2D calculations and for 1D calculations $r_0=75$ bohr. The TDSE (equation (9)) was solved by a 3rd order split step method [36, 37], starting from the ground state of the model Ne atom. The ground state was found by representing field-free Hamiltonian in matrix form on the Cartesian spatial grid,

and diagonalizing it. The temporal envelope of the electric field was an amplitude trapezoid with a five-cycle long flat top section and five-cycle long rise and fall sections. 2D calculations were carried out on a square Cartesian spatial grid, spanning from $x_{\min}, y_{\min} = -60$ bohr to $x_{\max} = y_{\max} = 60$ bohr, with a grid spacing of $dx = dy = 0.0586$ bohr and a timestep of $dt = 0.011$. The dipole acceleration was calculated by Ehrnfest's theorem:

$$\mathbf{a}(t) = -\langle \psi(\vec{r}, t)| \nabla V(r) + \mathbf{E}(t) |\psi(r, t)\rangle. \tag{12}$$

From which, the harmonic spectra were obtained by a Fourier transform

$$\widetilde{\boldsymbol{E}}(n\omega) = F \cdot T\{\mathbf{a}(t)\}. \tag{13}$$

Author contributions

All authors made substantial contributions to all aspects of the work.

Conflict of interests

The authors declare no competing interests.

Data availability statement

The data that support the findings of this study are available upon reasonable request from the authors.

Acknowledgments

This work was supported by the Israel Science Foundation (Grant No. 1781/18). O N gratefully acknowledges the support of the Adams Fellowship Program of the Israel Academy of Sciences and Humanities and support from the Alexander von Humboldt foundation.

ORCID iDs

Matan Even Tzur https://orcid.org/0000-0002-3777-6123
Ofer Neufeld https://orcid.org/0000-0002-5477-2108

References

[1] Holthaus M 2015 *J. Phys. B: At. Mol. Opt. Phys.* **49** 013001
[2] Lindner N H, Refael G and Galitski V 2011 *Nat. Phys.* **7** 490
[3] Katan Y T and Podolsky D 2013 *Phys. Rev. Lett.* **110** 016802
[4] Fleury R, Khanikaev A B and Alù A 2016 *Nat. Commun.* **7** 1
[5] Rechtsman M C, Zeuner J M, Plotnik Y, Lumer Y, Podolsky D, Dreisow F, Nolte S, Segev M and Szameit A 2013 *Nature* **496** 196
[6] Lu L, Joannopoulos J D and Soljačić M 2014 *Nat. Photon.* **8** 821
[7] Leykam D, Rechtsman M C and Chong Y D 2016 *Phys. Rev. Lett.* **117** 013902
[8] Lustig E, Weimann S, Plotnik Y, Lumer Y, Bandres M A, Szameit A and Segev M 2019 *Nature* **567** 356
[9] Ben-Tal N, Moiseyev N and Beswick A 1993 *J. Phys. B: At. Mol. Opt. Phys.* **26** 3017
[10] Alon O E, Averbukh V and Moiseyev N 1998 *Phys. Rev. Lett.* **80** 3743
[11] Morimoto T, Po H C and Vishwanath A 2017 *Phys. Rev.* B **95** 195155
[12] Neufeld O, Podolsky D and Cohen O 2019 *Nat. Commun.* **10** 1
[13] Long S, Becker W and McIver J K 1995 *Phys. Rev.* A **52** 2262
[14] Fleischer A, Kfir O, Diskin T, Sidorenko P and Cohen O 2014 *Nat. Photon.* **8** 543
[15] Kfir O *et al* 2015 *Nat. Photon.* **9** 99
[16] Baykusheva D, Ahsan M S, Lin N and Wörner H J 2016 *Phys. Rev. Lett.* **116** 123001
[17] Frumker E *et al* 2012 *Phys. Rev. Lett.* **109** 233904
[18] Kraus P M, Rupenyan A and Wörner H J 2012 *Phys. Rev. Lett.* **109** 233903
[19] Neufeld O, Ayuso D, Decleva P, Ivanov M Y, Smirnova O and Cohen O 2019 *Phys. Rev.* X **9** 031002
[20] Neufeld O and Cohen O 2019 *Phys. Rev. Lett.* **123** 103202
[21] Vampa G *et al* 2018 *Nat. Photon.* **12** 465
[22] Silva R E F, Jiménez-Galán Á, Amorim B, Smirnova O and Ivanov M 2019 *Nat. Photon.* **13** 849
[23] Dahlström J M, L'Huillier A and Maurits son J 2011 *J. Phys. B: At. Mol. Opt. Phys.* **44** 095602
[24] Shafir D, Soifer H, Bruner B D, Dagan M, Mairesse Y, Patchkovskii S, Ivanov M Y, Smirnova O and Dudovich N 2012 *Nature* **485** 343
[25] Rodriguez-Vega M, Lentz M and Seradjeh B 2018 *New J. Phys.* **20** 093022

[26] Aidelsburger M, Nascimbene S and Goldman N 2018 *C. R. Phys.* **19** 394
[27] Hübener H, De Giovannini U and Rubio A 2018 *Nano Lett.* **18** 1535
[28] Lewenstein M, Balcou P, Ivanov M Y, L'Huillier A and Corkum P B 1994 *Phys. Rev.* A **49** 2117
[29] Fleischer A and Moiseyev N 2005 *Phys. Rev.* A **72** 032103
[30] Bordo E, Kfir O, Zayko S, Neufeld O, Fleischer A, Ropers C and Cohen O 2020 *J. Phys. Photon.* **2** 034005
[31] Barreau L *et al* 2018 *Nat. Commun.* **9** 4727
[32] Lysne M, Murakami Y, Schüler M and Werner P 2020 *Phys. Rev.* B **102** 081121
[33] Shin D, Hübener H, De Giovannini U, Jin H, Rubio A and Park N 2018 *Nat. Commun.* **9** 638
[34] Cenker J *et al* 2021 *Nat. Phys.* **17** 20
[35] Neufeld O, Fleischer A and Cohen O 2019 *Mol. Phys.* **117** 1956
[36] Fleck J A, Morris J R and Feit M D 1976 *Appl. Phys.* **10** 129
[37] Feit M D, Fleck J A Jr and Steiger A 1982 *J. Comput. Phys.* **47** 412